Traffic 2009; **10:** 1019–1033

doi: 10.1111/j.1600-0854.2009.00932.x

Functional Rescue of β_1-Adrenoceptor Dimerization and Trafficking by Pharmacological Chaperones

Hiroyuki Kobayashi[1], Koji Ogawa[1], Rong Yao[2], Olivier Lichtarge[2] and Michel Bouvier[1]*

[1] Département de Biochimie, Groupe de Recherche Universitaire sur le Médicament and Institut de recherche en Immunologie et en Cancérologie, Université de Montréal, Montréal, Québec, H3C 3 J7 Canada
[2] Molecular and Human Genetics, Baylor College of Medicine, Houston, TX 77030, USA
**Corresponding author: Michel Bouvier, michel.bouvier@umontreal.ca*

Site-directed mutagenesis guided by evolutionary trace analysis revealed that substitution of V179 and W183 within a cluster of evolutionarily important residues on the surface of the fourth transmembrane domain of the β_1-adrenergic receptor (β_1AR) significantly reduced the propensity of the receptor to self-assemble into homodimers as assessed by bioluminescence resonance energy transfer in living cells. These results suggest that mutation of V179 and W183 result in conformational changes that reduce homodimerization either directly by interfering with the dimerization interface or indirectly by causing local misfolding that result in reduced self-assembly. However, the mutations did not cause a general misfolding of the β_1AR as they did not prevent heterodimerization with the β_2AR. The homodimerization-compromised mutants were significantly retained in the endoplasmic reticulum (ER) and could not be properly matured and trafficked to the cell surface. Lipophilic β-adrenergic ligands acted as pharmacological chaperones by restoring both dimerization and plasma membrane trafficking of the ER-retained dimerization-compromised β_1AR mutants. These results clearly indicate that homodimerization occurs early in the biosynthetic process in the ER and that pharmacological chaperones can promote both dimerization and cell surface targeting, most likely by stabilizing receptor conformations compatible with the two processes.

Key words: β_1-adrenergic receptor, BRET, dimerization, endoplasmic reticulum, G protein-coupled receptor, pharmacological chaperone

Received 22 August 2008, revised and accepted for publication 24 April 2009

G protein-coupled receptors (GPCRs) represent the largest family of cell surface proteins involved in signal transduction. They direct responses to a wide variety of stimuli including light, odors, tastants, hormones and neurotransmitters and, as such, represent major targets for the development of drugs in most therapeutic indications. GPCRs are synthesized by membrane-bound polyribosomes and co-translationally translocated into the membrane of the endoplasmic reticulum (ER). Although generally referred to as a constitutive secretory pathway, the plasma membrane targeting of GPCRs is a tightly regulated process. Folding of the receptor in the ER and its exit to the Golgi represent the limiting steps in their maturation and cell surface expression (1). General molecular chaperones involved in the folding of many membrane proteins have been suggested to play important roles at different steps of this process (2–8). More specialized chaperones and escort proteins have also been found to be involved for specific GPCRs (9–15).

In addition to these interactions with general or specialized chaperones, homo- and heterodimerization of GPCRs have also been proposed to play a role in their folding and export to the cell surface. The most dramatic demonstration to date for a role of dimerization in GPCR cell surface trafficking comes from studies on a member of the family C GPCRs, the metabotropic $GABA_B$ receptor ($GABA_B$), demonstrating that heterodimerization between $GABA_{B1}$ and $GABA_{B2}$ is essential for proper targeting of a functional $GABA_B$ to the plasma membrane (16). In that case, dimerization involving a coiled–coil interaction between the carboxyl tails of the two receptors is necessary to hide an ER retention signal located in the cytoplasmic tail of $GABA_{B1}$ thus permitting the targeting of the dimeric receptor at the cell surface.

Although no such ER retention signal or direct evidence for coiled–coil interaction of their carboxyl tails were found for family A GPCRs, increasing data suggest that homo- and heterodimerization of members of family A GPCRs can also occur in the ER and be involved in receptor biogenesis and quality control of newly synthesized receptors (17). For example, mutations that were found to prevent homodimerization of the β_2-adrenergic receptors (ARs) (18) or the α_{1b}AR (19,20) also led to their retention in the ER, suggesting a link between dimerization and ER exit. Also, heterodimerization with either the α_{1b}AR (21) or the β_2AR (22) has been proposed to be necessary for the cell surface trafficking of the α_{1d}AR. However, the lack of knowledge about the molecular determinants of class A GPCR dimerization has limited our ability to explore the links between receptor dimerization and their trafficking.

For class A GPCRs, information gathered from cross-linking studies of the D2 dopamine receptor (23,24), transmembrane (TM) domain competition for the β_2-adrenergic, D2 dopamine and α_{1b}-adrenergic receptors (25–27), as

well as site-directed mutagenesis of the α-mating factor, β_2-adrenergic, CCR5 chemokine and α_{1b}-ARsβ_2-adrenergic, CCR5 chemokine and α_{1b}-adrenergic receptors(18,19,28,29), suggested the involvement of various TM domains in the dimerization process (helix I and IV being most frequently implicated). Although these studies provided information about potential domains involved in class A GPCR self-assembly, much remains to be learned about the structural organization of the dimers and in particular concerning the specific residues involved in the dimerization interfaces for different receptors.

One bioinformatics approach recently developed to identify residues that may play important roles in protein structure, function or defining specific protein–protein interaction is known as evolutionary trace (ET) analysis. ET exploits the fact that the sequence variations of functional site residues tend to correlate more tightly with evolutionary divergences than residues with lesser functional impact (30). As a result, sequence analysis may be combined with protein structure information to rank residues by the extent of their phylogenetic correlation and then identify geometric clusters of top-ranked residues that may then predict functional sites in the protein structure that are common to the entire protein family (31). The identification of such clusters has successfully allowed the unraveling of important functional domains in several classes of proteins (32,33). Particularly relevant to the present study, clusters of residues on the surface of proteins have been proposed to be likely sites for protein–protein interaction (34) and thus could be involved in oligomerization processes. It should also be noted that studies targeting substitutions of top-ranked ET residues repeatedly enabled modulation of function (35–39) or separation of function (33,40), suggesting that specific sites could be altered or blocked through point mutations without leading to global perturbation of the protein fold.

In recent years, treatment with pharmacological chaperones has been shown to rescue the proper plasma membrane targeting of mutant forms of GPCRs that are otherwise retained in the ER (41). By binding to the intracellularly retained receptors, these lipophilic ligands are believed to stabilize receptor conformations that can then enable them to escape from the ER quality control system, reach the plasma membrane and be functional. In the cases of GPCR mutations leading to disease as a result of ER retention, pharmacological chaperones represent promising therapeutic avenues (42–44). In the context of studying the link between folding, dimerization and cell surface targeting, pharmacological chaperones could represent useful tools for the design of gain of function experiments whereby the effects of pharmacological chaperones could be assessed on both the propensity of the receptor to self-assemble and to be trafficked to the cell surface.

In this context, we used ET analysis to guide site-directed mutagenesis aimed at identifying residues involved in the homodimerization of the class A GPCR β_1AR and tested the effect of mutating these residues on both dimerization and receptor trafficking. The ability of lipophilic β-adrenergic ligands to act as pharmacological chaperones on the ER-retained dimerization-compromised β_1AR mutants was also assessed.

Results

To identify sites that could be important in directing protein–protein interactions of bioamine class A GPCRs, 139 receptor sequences, including 26 β-adrenergic, 29 α-adrenergic, 30 serotonergic, 30 dopaminergic, 18 cholinergic muscarinic and 6 histaminic GPCRs, were traced with the ET method (30,45). The list and accession number of all sequences used for the analysis are provided in the Supporting Information Table S1. The analysis was restricted to the TM domains because of their proposed role in dimerization and to reduce confusion that could result from the identification of domains involved in interactions with cytoplasmic and extracellular receptor partners. The ET produces a relative ranking of evolutionary importance among residues, where 1 is best and indicates absolute invariance (46). TM residues ranking in the top 50% mapped mostly to the structural core of the receptor (47), but some of these residues also delineated three clusters on the outward, lipid-facing surface of the receptor (Figure 1). The first cluster included residues in TM2, TM3 and TM4 whereas the other two were composed of residues within TM5, TM6 and TM7. Because several conserved residues within clusters 2 and 3 have been proposed to be important for ligand binding and signaling functions for many class A GPCRs (48–53), we focused our search for putative protein–protein interaction sites in cluster 1 to avoid possible confounding effects that could result from mutating residues directly involved in ligand binding and signaling. Four residues with different relative ET rankings (L105, V179. W183, I194) were selected for mutagenesis. Their positions on the surface of the β_1AR as well as their ET rankings are shown in Figure 1. To make sure that the mutations would result in significant modification of the protein surface shape, we replaced the aliphatic residues (e.g., leucine, isoleucine, and valine) with bulky aromatic amino acids (e.g., tryptophan or phenylalanine) and the bulky tryptophan residue by the small alanine.

To assess the effect of the selected mutations on receptor dimerization, bioluminescence resonance energy transfer (BRET) studies assessing the propensity of the receptor to self-assemble were carried out. For this purpose, wild type (WT) and mutant forms of the β_1AR were fused to the energy donor, *Renilla* luciferase (*R*luc), and the blue-shifted green fluorescent protein (GFP-10) (54) energy acceptor. GFP10- and *R*luc-fused WT or mutant receptors were then co-expressed in HEK293 cells, and the occurrence of BRET determined and used as a reporter for receptor self-assembly. BRET experiments

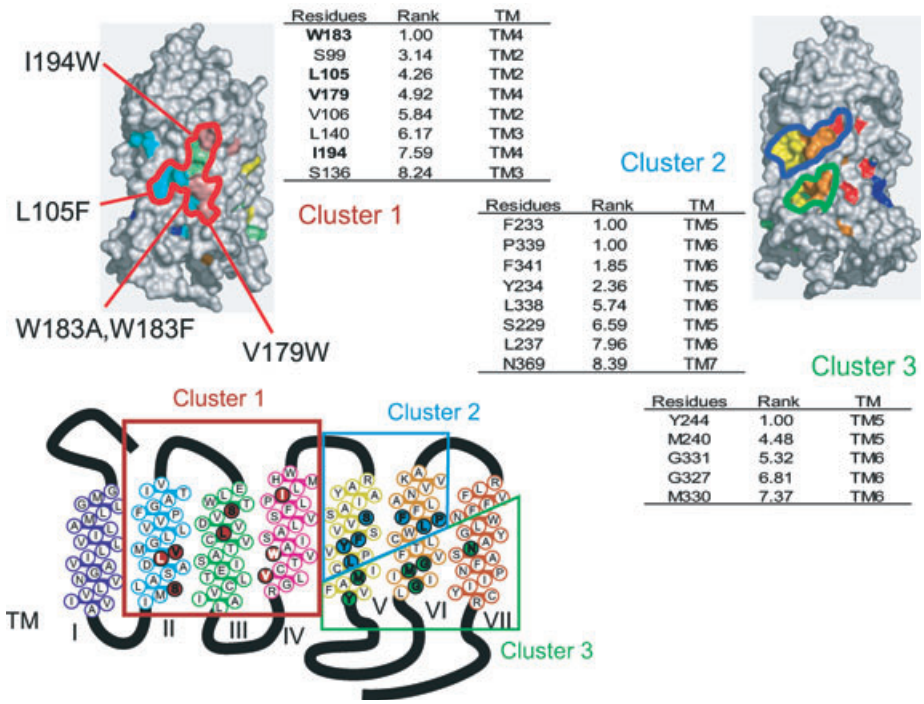

Figure 1: Evolutionary conserved residues on the surface of monoamine GPCR TM domains deduced from ET analysis. The trace residue clusters identified correspond to group of residues ranking into the top 50% of the ET analysis that map onto specific surface domains of the receptor. The ranking of each residue represents relative evolutionary importance, where 1 indicates absolute invariance. Three significant clusters were identified: cluster 1 includes residues spanning TM 2, TM3 and TM4, whereas clusters 2 and 3 are composed of residues within TM5, TM6 and TM7. The residues numbering corresponds to the position within the human β_1AR.

were performed in a titration format, where the amount of transfected β_1AR-*R*luc is maintained constant while the amount of β_1AR-GFP10 is gradually increased, allowing to assess the relative propensity of WT versus mutant receptors to self-assemble (18,55). As shown in Figure 2A, the BRET signal between β_1AR-*R*luc and β_1AR-GFP10, expressed as a function of the GFP10/*R*luc ratios, increased hyperbolically as a function of the increased expression of β_1AR-GFP10. The selectivity of the signal observed is illustrated by the reduction in the BRET signal observed upon co-expression of hemagglutin (HA)-tagged β_1AR (not fused to either *R*luc or GFP10) that act as a BRET competitor by interacting with either β_1AR-*R*luc or β_1AR-GFP10, thus preventing interaction between the BRET partners and blunting the energy transfer (Supporting Information Figure S1).

From the BRET titration curves, $BRET_{50}$ values corresponding to the concentration of β_1AR-GFP10 needed to generate 50% of the maximal BRET signal were used as

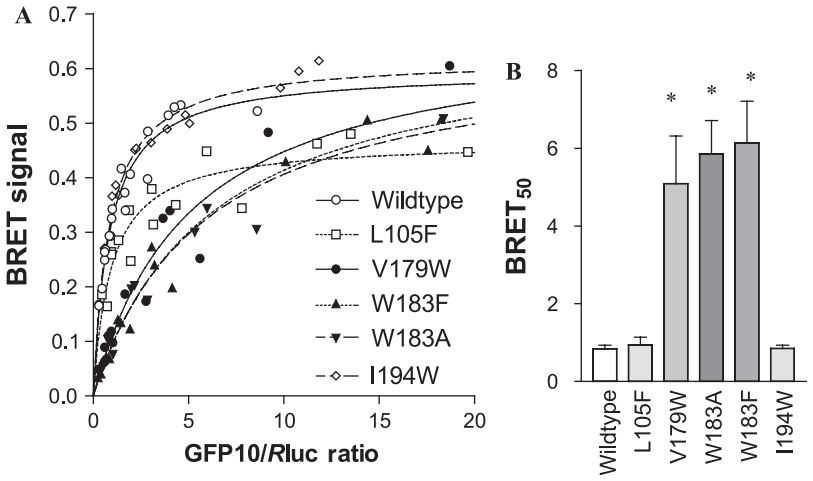

Figure 2: BRET titration analysis of β_1AR self-assembly. Cells were co-transfected with fixed amount of β_1AR-*R*luc and increasing amounts of β_1AR-GFP10. Both the *R*luc-tagged and the GFP10-tagged β_1AR are carrying the indicated mutations. A) BRET signals are plotted as a function of the ratio between total fluorescence (GFP) and total luminescence (*R*luc), indicative of the energy acceptor/donor ratio. Values shown represent combined data from three to four independent experiments for each pair. B) $BRET_{50}$ represent the GFP/*R*luc ratio leading to 50% of the maximal BRET signal and were calculated from BRET titration curve fitting using non-linear regression of three to four independent experiments. $^*p < 0.01$.

an index of the relative propensity of the protomers to self-assemble. As can be seen in Figure 2, mutations of L105 and I194 to phenylalanine and tryptophan residues, respectively (L105F, I194W), modestly reduced the maximal BRET signal but did not affect the $BRET_{50}$ value, indicating that these mutations did not significantly affect the dimerization propensity of the β_1AR. In contrast, mutations of V179 and W183 to tryptophan and alanine residues, respectively (V179W, W183A), caused a significant ($P < 0.01$) rightward shift of the BRET titration curves (Figure 2A), resulting in 6.1- and 7.0-fold higher $BRET_{50}$ values when compared with WTβ_1AR (Figure 2B). Mutation of W183 to a phenylalanine residue (W183F) led to a similar (7.3-fold) increase in $BRET_{50}$ value, indicating that substituting a residue smaller than the tryptophan but significantly bulkier than alanine was sufficient to promote the decrease in protomers self-assembly. The increased $BRET_{50}$ did not result from non-specific destabilization of the protein because destabilizing mutations should equally affect the receptor fused to the donor and acceptor, and thus should not affect the relative acceptor/donor concentration and hence not change the $BRET_{50}$. Therefore, our results suggest that mutations at positions V179 and W183 in TM4 decrease the propensity of the receptor to self-assemble into a dimer.

Combining the two mutations in the same construct, led to further disruption of the receptor self-assembly as reflected by the much smaller BRET signals and a titration curve that did not converge to an asymptote (Supporting Information Figure S2), indicating that this double mutant receptor could not dimerize and that the small BRET signal observed represented non-saturable random collision events known as bystander BRET (55). This double mutation also resulted in greater protein instability and was not studied any further because of its low steady-state expression levels.

In all BRET titration experiments, the expression levels of the β_1AR-*R*luc and β_1AR-GFP10 constructs were monitored by measuring the total luminescence and fluorescence signals. These signals can then be transformed into femtomoles of receptors/sample using titration curves correlating the luminescence and fluorescence signals to the number of receptor binding sites as determined by radioligand binding assays using [^{3}H]-dihydroalprenolol as the tracer (Supporting Information Figure S3). The titration experiments were designed to compare BRET values generated over similar acceptor/donor (GFP10/*R*luc) ratios but the absolute total number of receptor expressed varied between the different constructs. The expression level distributions for the WT and all mutants are presented in Supporting Information Figure S4. Although BRET signals are largely determined by the energy donor/acceptor ratios, they can also be influenced by the density of the partner proteins (55,56). As shown in Supporting Information Figure S4, the expression levels for V179Wβ_1AR, W183Fβ_1AR and W183Aβ_1AR were significantly lower than that of the WT receptor. Thus, to exclude a possible role of receptor density on the detected increase in $BRET_{50}$, additional transfection conditions were chosen to generate equivalent expression levels for the WT- and W183Aβ_1AR. In BRET titration experiments shown in Figure 3, the WT- and W183Aβ_1AR expression levels varied between 14–402 and 10–636 fmol, respectively. As was the case in Figure 2, the titration curve for W183Aβ_1AR was significantly right-shifted compared with that of the WT receptor, yielding an 8.1 × higher $BRET_{50}$. This confirmed that the increase in $BRET_{50}$ resulted from a reduced propensity of the mutant receptor to self-assemble and not from reduced receptor expression levels. Given that homodimerization of the β_1AR can be detected at physiological expression levels as low as 100 fmol/mg of protein, these results also demonstrate that dimerization does not result from forced interactions caused by receptor over-expression. The representation of the BRET curve as a function of GFP10/*R*luc molar ratios (deduced from the standard curves shown in Supporting Information Figure S3) also revealed that BRET was detected at very low molar ratio of energy donor/acceptor ($BRET_{50}$ molar ratio of 0.6 for WT β_1AR), which is consistent with the occurrence of constitutive homodimerization.

To assess whether the mutation is needed on each protomer to affect self-assembly, we then assessed the influence of the W183A mutation on the ability of the

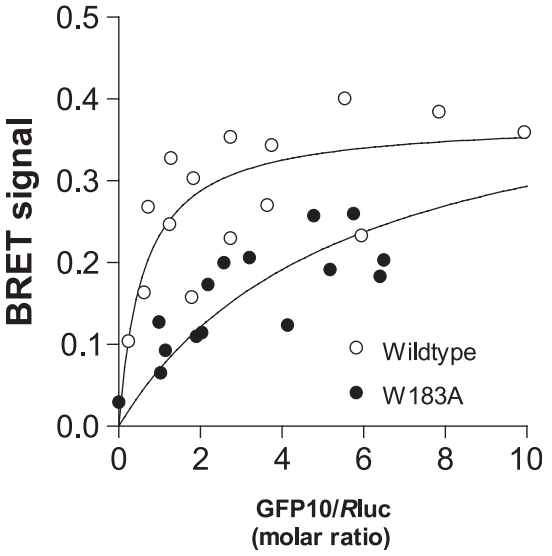

Figure 3: BRET titration analysis of WTβ_1AR and W183Aβ_1AR expressed at similar levels. Cells were co-transfected with fixed amount of WT- or W183Aβ_1AR-*R*luc and increasing amounts of WT- or W183Aβ_1AR-GFP10, respectively. Transfection conditions were selected to allow similar expression levels for WTβ_1AR (14–402 fmol/sample) and W183Aβ_1AR (10–636 fmol/sample). BRET signals are expressed as a function of receptor-GFP10/receptor-*R*luc molar ratios deduced from standard curves such as those presented in Figure S3. $BRET_{50}$ values were as follow: WTβ_1AR, 0.6 (CI 95%, 0.03–1.2); W183Aβ_1AR, 5.5 (CI 95%, 1.6–9.5).

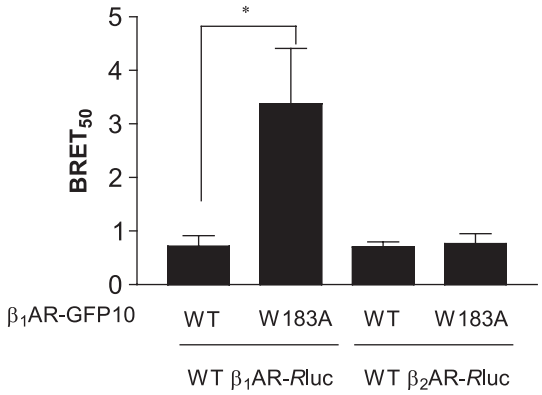

Figure 4: Influence of W183Aβ_1AR mutation on its interaction with WTβ_1AR and WTβ_2AR. Cells were co-transfected with fixed amount of WTβ_1AR-*R*luc or WTβ_2AR-*R*luc and increasing amount of WT- or W183Aβ_1AR-GFP10. BRET titration curves were generated for each pair by combining data of three to four independent experiments and were used to calculate $BRET_{50}$ values for each pairs using non-linear regression. The luciferase and fluorescence levels reached in these experiments were similar for each conditions (β_1AR-*R*luc = 491 ± 83 fmol; β_2AR-*R*luc = 583 ± 101 fmol; WTβ_1AR-GFP10 = 0–2039 fmol; W183Aβ_1AR-GFP10 = 0–1420 fmol). $^*p < 0.001$.

receptor to interact with either WTβ_1AR or the β_2AR that is known to heterodimerize with the β_1AR (55). As can be seen in Figure 4, the W183Aβ_1AR mutation significantly inhibited the ability of the receptor to interact with the WTβ_1AR, as illustrated by the 4.7-fold increase in $BRET_{50}$. However, the mutation did not affect the ability of the β_1AR to heterodimerize with the WTβ_2AR, as indicated by the identical $BRET_{50}$ values obtained for the WTβ_2AR-*R*luc/W183Aβ_1AR-GFP10 and WTβ_2AR-*R*luc/WTβ_1AR-GFP10 pairs. The observation that the mutation affected assembly with the WTβ_1AR but not WTβ_2AR indicates that mutation of W183 within a single protomer is sufficient to affect β_1AR homodimerization but not β_1AR/β_2AR heterodimerization, and thus that β_1AR homo- and heterodimerization may involve distinct domains and/or that the conformational changes promoted by the mutation affected the homodimerization but not the heterodimerization interface. This preserved ability of W183Aβ_1AR to hetrerodimerize with β_2AR also suggests that if the decreased propensity of the β_1AR to homodimerize resulted from local misfolding, the mutation did not lead to a global destructuration of the receptor organization.

We next examined the effects of the cluster 1 mutations on the subcellular distribution of the β_1AR-eGFP constructs by fluorescence confocal microscopy. As for the WT receptor, mutant β_1ARs that preserved their propensity to self-assemble (L105F and I194W) were largely found at the cell surface. In contrast, mutations that reduced receptor dimerization (V179W, W183F and W183A) lead to intracellular retention of the receptor (Figure 5). It was previously reported that cell-permeable ligands can rescue cell surface expression of ER-retained GPCRs through their action as pharmacological chaperones that bind to the neo-synthesized receptors and favor their export from the ER (42). Although no pharmacological chaperone has been described for the β_1AR yet, the fact that the high affinity β-adrenergic antagonist alprenolol can readily permeate lipid membranes makes it a likely candidate as a β_1AR pharmacological chaperone. We thus assessed whether treatment with alprenolol could rescue cell surface targeting of W183Aβ_1AR. As can be seen in Figure 6A, in the absence of treatment, W183Aβ_1AR is largely retained inside the cell where it co-localizes with the ER-resident protein, calnexin, confirming that the major

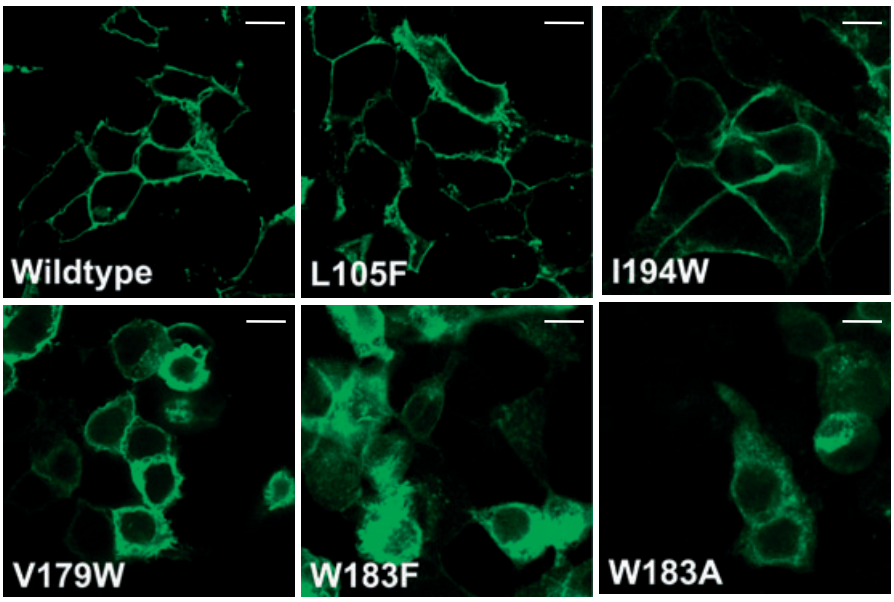

Figure 5: Subcellular distribution of WT and mutant β_1ARs. Cells were transfected with WT or the indicated mutant forms of β_1AR-eGFP and, 48 h post-transfection, cells were fixed and direct eGFP fluorescence was detected by confocal fluorescence microscopy. The confocal images show the subcellular distribution of WT, L105F, I194W, V179W, W183F and W183Aβ_1AR. The bar = 10 μm.

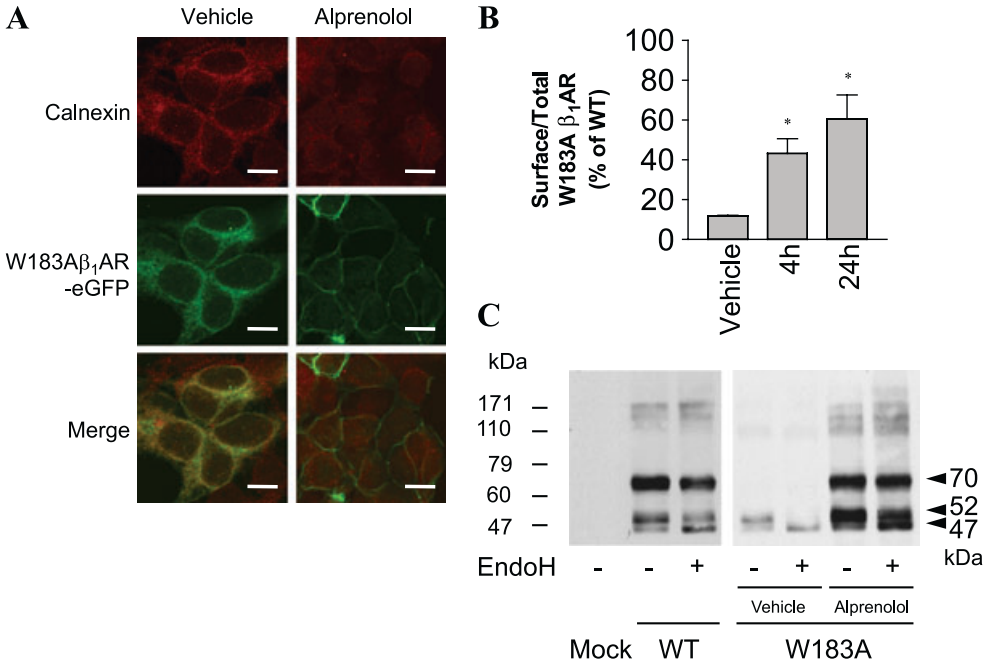

Figure 6: Influence of alprenolol treatment on the subcellular distribution and maturation of W183Aβ_1AR. A) Cells expressing W183Aβ_1AR-eGFP were treated or not with 10 μM alprenolol for 24 h, labeled with anti-calnexin antibody as a marker of the ER and prepared for confocal fluorescence microscopy. Confocal images show the localization of W183Aβ_1AR (green) and calnexin (red) and their merged co-localization (yellow). The bar = 10 μm. B) Cells expressing HA-β_1AR-*R*luc were treated or not with 10 μM alprenolol for 4 or 24 h. Cells were then split and either labeled with anti-HA antibody for cell surface (ELISA) detection or exposed to 5 μM coelenterazine h for detection of total expression (luminescence). The cell surface immunoreactivity/luciferase activity ratio was used as an index of the fraction of the total β_1AR population that was targeted at the cell surface. The data are expressed as percentage of the cell surface fraction observed for the WT receptor and represent the mean ± SEM of three independent experiments. $^*p < 0.01$. C) Cells expressing WT or mutant HA-β_1AR were treated or not with 10 μM alprenolol for 16 h. Receptors were immunoprecipetated with a mouse anti-HA antibody, treated or not with endoH, resolved on SDS-PAGE and immunoblotted with a rat anti-HA antibody. The data shown are representative of three independent experiments.

site of retention of the dimerization-compromised mutant is the ER. Treatment of the cells for 24 h with alprenolol favored the plasma membrane targeting of W183Aβ_1AR, as indicated by the clear redistribution of receptor labeling from the ER to the cell surface. To quantify the subcellular redistribution promoted by alprenolol, the proportion of the total receptor population expressed at the cell surface was determined by a ratiometric enzyme-linked immunosorbent assay (ELISA)/luciferase activity assay. For this purpose, a W183Aβ_1AR construct harboring an HA epitope at its extracellular N-terminal and *R*luc at its intracellular C-terminal (HA-W183Aβ_1AR-*R*luc) was used. HA-immunoreactivity detected in non-permeabilized cells is used as an indicator of cell surface receptor expression, whereas the luciferase activity measured upon addition of the cell-permeable substrate, coelenterazine h, reflects the total receptor expression. The immunoreactivity/luciferase ratio is then used as an index of the cell surface targeting efficacy. As shown in Figure 6B, the surface targeting efficacy of W183Aβ_1AR was 11 ± 0.36% of that of WTβ_1AR under control conditions. This efficacy was restored to 43 ± 7.4 and 60 ± 12% of that of the WT following alprenolol treatment for 4 and 24 h, respectively.

The ability of alprenolol to act as a pharmacological chaperone for W183Aβ_1AR was further investigated by assessing the effect of alprenolol on the maturation state of the receptor. As shown in Figure 6C, western blot analysis of β_1AR reveals three major bands at 47, 52 and 70 kDa. The 52 kDa core-glycosylated form that can be deglycosylated by endoglycosidase H (endoH) treatment represents the precursor form of the receptor before it exits the ER. The 70 kDa form, resistant to endoH treatment, corresponds to the mature receptor with complex sugar acquired in the Golgi, whereas the 47 kDa form observed in the absence of endoH treatment most likely represents a deglycosylated form of the receptor targeted for degradation (1). This deglycosylated form becomes more abundant following treatment with endoH as a result of the deglycosylation of the 52 kDa species. Fainter and poorly resolved bands above 110 kDa most likely represent residual dimeric receptor forms that resisted SDS denaturation. When considering W183Aβ_1AR, only the core-glycosylated immature and deglycosylated forms of the receptor are observed. This is consistent with the confocal microscopy images indicating that the mutation leads to retention of the receptor in the ER. Alprenolol treatment considerably stabilized

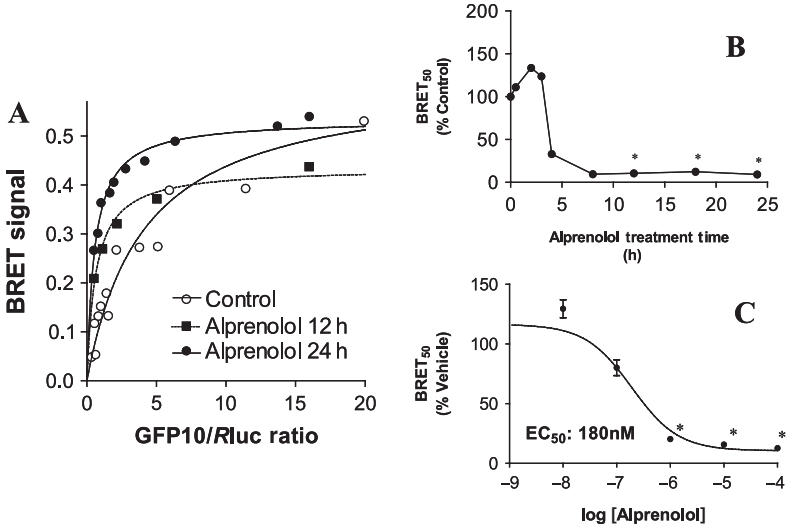

Figure 7: Influence of alprenolol on the self-assembly of W183Aβ_1AR. Cells were co-transfected with fixed amount of W183Aβ_1AR-*R*luc and increasing amount of W183Aβ_1AR-GFP10. A) Cells were treated or not with 10 μM alprenolol for 2–24 h and BRET levels were measured 48 h post-transfection. The BRET titration curves are plotted as in Figure 2. B) The $BRET_{50}$ values obtained from the curves in A for the different alprenolol treatment time are expressed as percentage of the $BRET_{50}$ value obtained in the absence of treatment. $^*p < 0.05$. C) Cells were treated with increasing concentration of alprenolol for 16 h. BRET values were measured as in A and $BRET_{50}$ values expressed as percentage of value obtained in the absence of treatment. Data are expressed as the mean ± SEM of three to five independent experiments. $^*p < 0.01$.

the W183Aβ_1AR precursor form, as can be seen by the increased immunoreactivity of the 52 kDa. More importantly, alprenolol favored ER exit as indicated by the appearance of the endoH resistant, fully glycosylated 70 kDa form of the receptor. Taken together, these results demonstrate that alprenolol acts as an efficacious pharmacological chaperone for the W183Aβ_1AR, most likely by binding to the mutant receptor in the ER and promoting its maturation.

To determine whether the maturation and cell surface expression rescue was accompanied by a change in the dimerization status of the receptor, we assessed the effect of alprenolol on the self-assembly propensity of W183Aβ_1AR by performing BRET titration curves. As shown in Figure 7A, treatment with alprenolol for extended periods of time significantly affected the curves. Treatments led to a time-dependent leftward shift in the BRET titration curves, yielding significant reduction in the $BRET_{50}$ values that became statistically significant following a 12-h treatment (Figure 7B), indicating that alprenolol increased the propensity of W183Aβ_1AR to dimerize. The small increase in $BRET_{50}$ observed after short time treatment with alprenolol did not reach statistical significance. Treatment with alprenolol also led to a significant increase in steady-state receptor levels, increasing from a range of 53–916 fmol/sample for titration curves performed in control conditions to a range of 452–1813 fmol/sample for titrations carried out following 12 or 24 h treatments with alprenolol. However, these changes in expression levels did not account for the decrease in $BRET_{50}$ ($BRET_{50}$: 4.1 in control condition; 0.56 following a 24-h treatment with alprenolol), because titration curves obtained from transfections covering similar ranges of expression levels for W183Aβ_1AR (10–636 versus 115–1968 fmol/mg) in the absence of treatment did not show any significant differences in $BRET_{50}$ (data not shown).

The ability of alprenolol to promote W183Aβ_1AR self-assembly was concentration dependent, with an EC_{50} value of 180 nM (Figure 7C). This EC_{50} value is somewhat higher than the binding affinity values obtained from radioligand binding assays (e.g., 3.9–4.2 nM, (57)). This difference is compatible with what was previously reported for the apparent potency of pharmacological chaperones that are generally lower than their binding affinities for the WT receptors (58,59). This lower apparent potency could reflect a loss of binding affinity for alprenolol resulting from a conformational effect of the mutation.

Interestingly, co-expression of the W183Aβ_1AR with the WTβ_2AR led to the intracellular retention of the latter (Figure 8A,B), presumably as a result of its association with the intracellularly retained mutant β_1AR. This confirms the preserved ability of W183Aβ_1AR to heterodimerize with the β_2AR. In contrast, co-expression of W183Aβ_1AR with WTβ_1AR did not lead to the retention of WTβ_1AR (Figure 8B), consistent with the decreased propensity of W183Aβ_1AR to associate with the WTβ_1AR (Figure 4; 4.7-fold increase in $BRET_{50}$ when compare with WTβ_1AR self-assembly). Although this reduced propensity was not as dramatic as the one observed for W183Aβ_1AR homodimerization (Figure 2; 7.0-fold increase in $BRET_{50}$), it was sufficient to prevent ER retention of WTβ_1AR. Treatment of cells co-expressing W183Aβ_1AR and WT β_2AR with alprenolol restored the plasma membrane targeting of the β_2AR (Figure 8A), most likely as a result of the rescue of the retained W183Aβ_1AR/β_2AR heterodimer. The co-expression of the β_2AR did not affect the dimerization pattern of either WTβ_1AR (Supporting Information Figure S5) or W183Aβ_1AR (Figure 8C). In addition, treatment with alprenolol promoted a reduction in the $BRET_{50}$ determined for W183Aβ_1AR-*R*luc/W183Aβ_1AR-GFP10 homodimer even in the presence of β_2AR. These results clearly indicate that the β_2AR does not compete with β_1AR homodimerization, consistent with the notion evoked earlier that β_1AR homodimerization and β_1/β_2AR

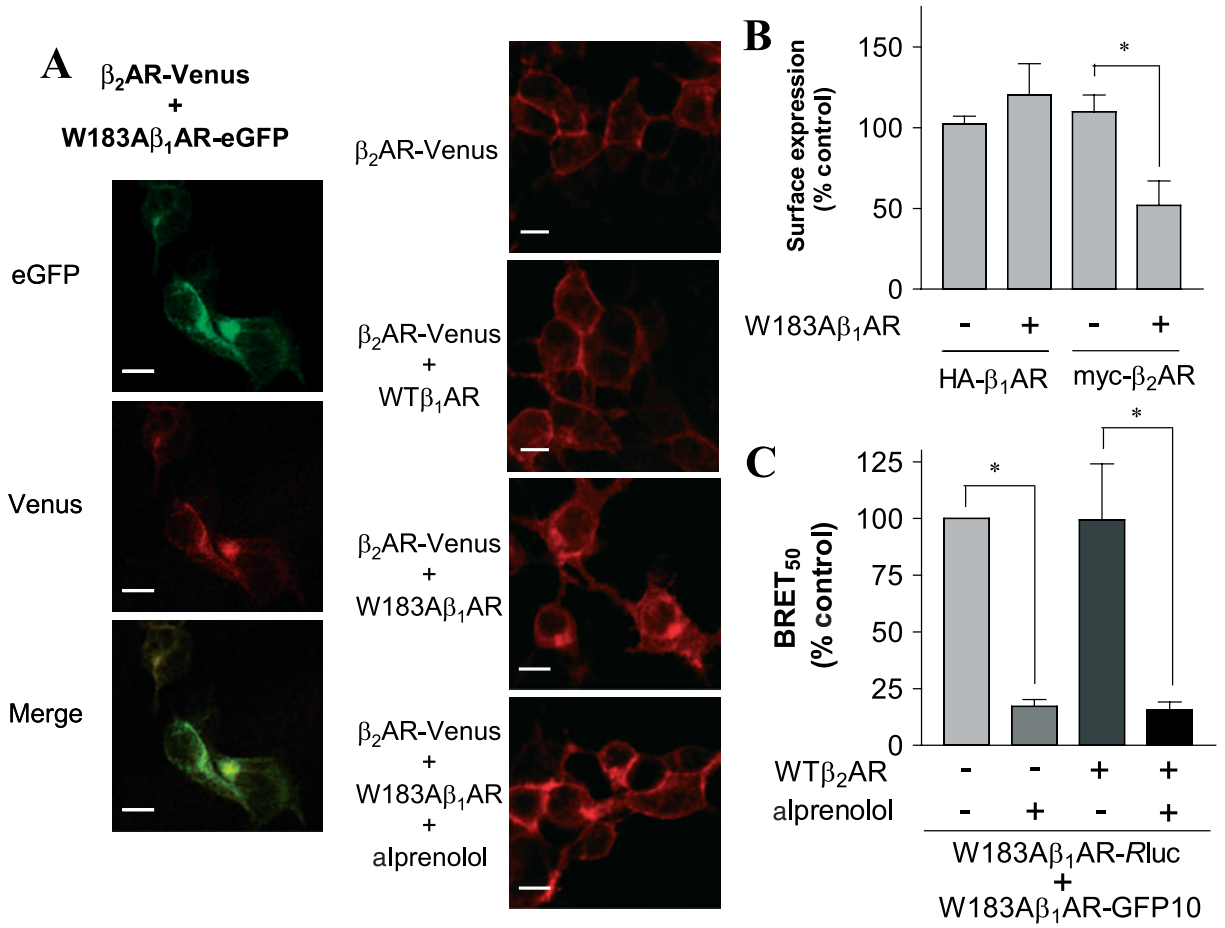

Figure 8: Influence of W183Aβ_1AR on the subcellular distribution of WTβ_2AR and effect of WTβ_2AR on the W183Aβ_1AR dimerization. A) Cells were transfected with WTβ_2AR-Venus alone or co-transfected in the presence of WTβ_1AR, W183Aβ_1AR or W183Aβ_1AR-eGFP and, 48 h post-transfection, cells were treated or not with 10 μM alprenolol for 16 h, and both eGFP and Venus fluorescence detected by confocal fluorescence microscopy. The confocal images on the left panel show subcellular distribution of WTβ_2AR (red) and W183Aβ_1AR-eGFP (green), as well as the co-localization of the two receptors (yellow). The images on the right panel show subcellular distribution of the WTβ_2AR in the presence or absence of WTβ_1AR, W183Aβ_1AR and alprenolol. The bar = 10 μm. B) Cells were transfected with HA-WTβ_1AR-Venus or myc-WTβ_2AR-Venus, in the presence or the absence of W183Aβ_1AR. Venus fluorescence was measured to determine total receptor expression level and cell surface receptors were detected with anti-HA or anti-myc antibody. The cell surface immunoreactivity/Venus fluorescence ratio was used as an index of the fraction of the total β_1AR/β_2AR population that is targeted at the cell surface. The data are expressed as percentage of the cell surface fraction observed in the absence of W183Aβ_1AR and represent the mean ± SEM of three independent experiments. *$p < 0.05$. C) Cells were co-transfected with fixed amount of W183Aβ_1AR-*R*luc and increasing amount of W183Aβ_1AR-GFP10, in the presence or absence of WTβ_2AR. BRET levels were measured following or not 16 h treatment of 10 μM alprenolol. $BRET_{50}$ values were calculated from BRET titration curves. Data are expressed as percentage of the $BRET_{50}$ observed in the absence of treatment and represent the mean ± SEM of three independent experiments. *$p < 0.05$.

heterodimerization probably involve distinct interfaces. The absence of competition between β_2AR and β_1AR homodimerization combined with the restored cell surface expression of the WTβ_2AR/W183Aβ_1AR heterodimer upon pharmacological chaperone treatment may suggest the existence of higher order oligomers composed of both β_1AR and β_2AR dimers, as was recently suggested for other class A receptors (60,61).

To test whether other β-adrenergic ligands could affect the dimerization propensity of W183Aβ_1AR, the effect of seven compounds was assessed on the $BRET_{50}$ of the W183Aβ_1AR-*R*luc/W183Aβ_1AR-GFP10 pair. Five of the seven compounds led to significant reductions in $BRET_{50}$ (Figure 9A). The only two compounds not affecting the BRET titration curve were isoproterenol and atenolol, two compounds with low hydrophobic character that most likely cannot penetrate lipid membranes. In fact, excellent correlations were found between the ability of the compounds to affect the self-assembly of the W183Aβ_1AR ($BRET_{50}$) and both their relative membrane permeability estimated by the calculated

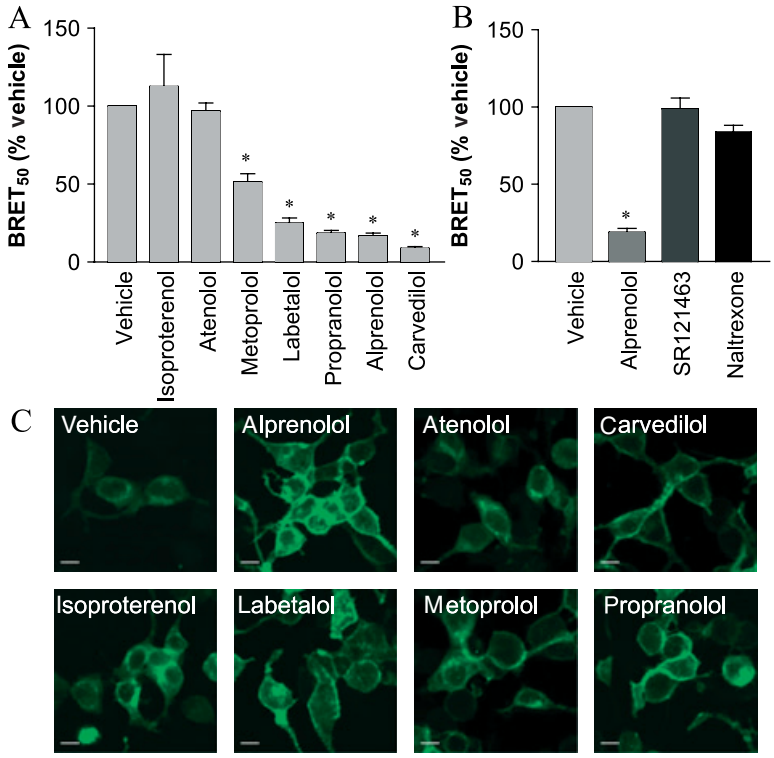

Figure 9: Effect of various ligands on the self-assembly and subcellular distribution of W183β_1AR. Cells were co-transfected with fixed amount of W183Aβ_1AR-*R*luc and increasing amount of W183Aβ_1AR-GFP10. A) BRET titration analyses were performed following a 16-h treatment with 10 μM of the indicated βAR ligands. B) BRET titration analyses were performed following a 16-h treatment with 10 μM alprenolol and lipophilic ligands previously shown to act as selective pharmacological chaperones for other GPCRs (SR121463; pharmacolocal chaperone for vasopressin V2 receptor and naltrexone; pharmacological chaperone for δ-opioid receptor). A, B) The $BRET_{50}$ obtained from the individual BRET titration curves are expressed as percentage of the $BRET_{50}$ value obtained in the absence of treatment. Data are expressed as the mean ± SEM of three independent experiments. $^*p < 0.05$. C) Cells were transfected with W183Aβ_1AR-eGFP. Fluorescence was detected by confocal fluorescence microscopy following a 16-h treatment with the indicated ligands: alprenolol, atenolol, carvedilol, isoproterenol, labetalol, metoprolol or propranolol). All βAR ligands were used at 10 μM. The bar = 10 μm.

logP ($r^2 = 0.82$) and their affinity for the β_1AR ($r^2 = 0.90$), consistent with the notion that the ligands need to penetrate the cell and bind the receptor to have their pharmacological chaperone action. The pharmacological selectivity of action is further illustrated by the observation that, in contrast to β-adrenergic ligands, treatments for 24 h with SR121463 or naltrexone, known pharmacological chaperones for the V2-vasopressin (58) and δ-opioid (59) receptors, respectively, did not affect the $BRET_{50}$ observed for the W183Aβ_1AR-*R*luc/W183Aβ_1AR-GFP10 pair (Figure 9B). Immunofluorescence microscopy revealed that the effect of the compounds on the $BRET_{50}$ is a good predictor of their ability to rescue cell surface expression of W183Aβ_1AR (Figure 9C). Indeed, isopreterenol, atenolol and metoprolol that had either no or modest effect on the $BRET_{50}$ did not readily promote detectable trafficking of the receptor to the cell surface whereas all other adrenergic compounds had robust effects on the $BRET_{50}$ and clearly restored cell surface expression.

To further explore whether the action of the pharmacological chaperone on dimerization occurs in the early phase of receptor ontogeny, we tested the effect of an inhibitor of ER-golgi transport, brefeldin A. By promoting the fusion of the cis-Golgi with the ER, brefeldin A treatment allows to assess whether the pharmacological chaperone can act on dimerization before trans-Golgi processing. As shown in Figure 10, a 6-h treatment with alprenolol led to a significant reduction of the $BRET_{50}$ for the W183Aβ_1AR-*R*luc/W183Aβ_1AR-GFP10 pair in the presence and absence of brefeldin A. Given that the brefeldin A treatment completely blocked the alprenolol-promoted cell surface targeting of the receptor (data not shown), these results indicate that alprenolol favors the

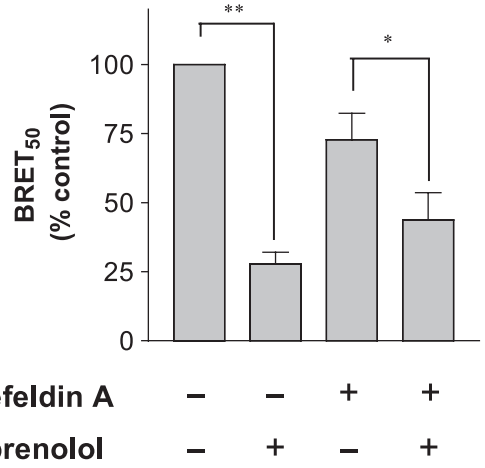

Figure 10: Influence of brefeldin A on the dimer promoting activity of alprenolol. Cells were co-transfected with fixed amount of W183Aβ_1AR-*R*luc and increasing amount of W183Aβ_1AR-GFP10. BRET levels were measured following a 6-h treatment in the presence or absence of 10 μM alprenolol and 5 μg/ml Brefeldin A, as indicated. $BRET_{50}$ values were calculated from BRET titration curves. Data are expressed as percentage of the $BRET_{50}$ observed in the absence of treatment and represent the mean ± SEM of three independent experiments. $^*p < 0.05$, $^{**}p < 0.001$.

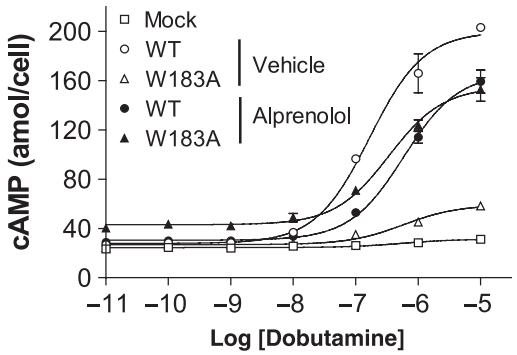

Figure 11: Influence of alprenolol pre-treatment on dobutamine-stimulated cAMP production. Cells expressing WT or W183Aβ_1AR were treated or not with 10 μM alprenolol for 16 h, washed extensively and treated with increasing concentration of dobutamine for 15 min. Cells were then lysed and intracellular cAMP concentration was determined. Data are expressed as the mean ± SEM of three independent experiments.

self-assembly of W183Aβ_1AR before it exit the cis-Golgi, most likely in the ER.

To verify whether the alprenolol-promoted dimerization and cell surface expression of the W183Aβ_1AR resulted into functionally active receptors, the ability of the selective β_1AR agonist dobutamine to stimulate cyclic AMP (cAMP) production was assessed. As shown in Figure 11, in the absence of alprenolol pre-treatment, dobutamine stimulated a robust concentration-dependent cAMP production in cells expressing the WTβ_1AR but only a very modest response at the highest agonist concentrations in cells expressing W183Aβ_1AR. This is consistent with the observation that W183Aβ_1AR is poorly targeted to the plasma membrane. In contrast, dobutamine promoted a similar concentration-dependent cAMP response for both WTβ_1AR and W183Aβ_1AR expressing cells following pre-treatment with alprenolol, indicating that, in addition to promote dimerization and cell surface targeting, the pharmacological chaperone action of alprenolol restored the signaling properties of W183Aβ_1AR. The somewhat smaller response observed in both WTβ_1AR and W183Aβ_1AR-expressing cells following alprenolol pre-treatment, when compared with non-pretreated WTβ_1AR-expressing cells, most likely results from incomplete washout of alprenolol before the dobutamine challenge.

Discussion

Our data clearly demonstrate that mutations of two residues (V179 and W183) located in TM4 of the β1AR had profound effects on the self-assembly capacity of the receptor. Substitution of V179 to tryptophan or of W183 to either alanine or phenylalanine significantly increase the $BRET_{50}$ of the β_1AR homodimer without affecting the maximal BRET signal reached. $BRET_{50}$ being a reflection of the protomers' propensity to self-assemble (55), it follows that V179W, W183A and W183F mutations most likely affected the ability of individual molecules of β_1AR to form dimers without completely inhibiting dimerization.

Although the mutated residues were identified as part of a cluster present at the surface of the receptor that could be involved in protein–protein interactions, our data do not allow to conclude that V179 and W183 are directly involved in the homodimerization interface. Indeed, conformational changes leading to local misfolding that indirectly affect dimerization could also underlie the effects of the mutations. In fact, the recently resolved crystal structure of the turkey β1AR (62) indicates that the residues corresponding to V179 and W183 in the human β1AR establish contact with the backbone of the TM2 and may stabilize the local orientation of the two TM surfaces. Mutation of these residues may thus locally destabilize the structure of the receptor. Consistent with such a conformational effect is the observation that the concentration of alprenolol required to act as a pharmacological chaperone on the mutant receptors is much higher than the affinity of the ligand for the WT receptor (180 versus 1–10 nM) indicating that the mutation may have indirectly affected the binding pocket. However, several lines of evidence indicate that the reduced homodimerization did not result from global receptor misfolding. First, W183Aβ_1AR preserved a normal ability to heterodimerize with the β_2AR indicating that the mutation selectively prevented homodimerization. Also, the mere fact that alprenolol, carvedilol, labetalol and propranolol acted as pharmacological chaperone indicates that the mutant receptor maintained a ligand binding pocket that allows binding, albeit maybe with lower affinity, of these small ligands. Finally, W183Aβ_1AR rescued by the pharmacological chaperone could efficiently respond to agonist stimulation by triggering G protein signaling. Nevertheless, whether the loss of dimerization resulted from the mutation of residues directly involved in the homodimerization interface or from local misfolding cannot be ascertain from our data.

Our results are in agreement with a growing consensus suggesting that TM4 residues may play important roles in class A GPCR dimerization (63). However, several other TM domains have also been proposed to participate into both homo- and hetero-oligomerization (23,26,27,64,65), and it is likely that several points of contact located on different TM domains contribute to the quaternary structure arrangements of receptor homo and heterodimers. It is also likely that different receptors may use distinct domains to dimerize. Consistent with this notion, mutation of W158 to alanine in the β_2AR (corresponding to W183 in the β_1AR) did not affect its homodimerization $BRET_{50}$ (data not shown). This could suggest that different receptors even as closely related as the β_1AR and β_2AR use different dimerization interfaces or that the mutation has different conformational consequences for β_1AR and β_2AR. The observation that over-expression of β_2AR did not compete with β_1AR homodimerization is consistent with the

first possibility. Clearly, additional work will be necessary to have a clearer picture of the three-dimensional organization of various homo and heterodimers.

Independent of the mechanism underlying the effect of the mutations on dimerization, our results clearly show that the three mutations affecting self-assembly of the β_1AR (V179W, W183A and W183F) also greatly reduced cell surface targeting of the receptor as a result of its retention in the ER. In contrast, mutations of the nearby residue I194 in TM4 (I194W) or L105 in TM2 (L105F), which did not affect dimerization, were without effect on receptor trafficking. This apparent correlation between dimerization propensity and ER-export is consistent with an increasing number of studies indicating that dimerization occurs in the ER for many class A GPCRs, including the β_2-adrenergic (18), vasopressin V2 (56), melanocortin MC1 (66) and serotonin $5HT_{2C}$ (67) receptors. In one of these studies, mutations in TM6 were found to reduce the propensity of the β_2AR to self-assemble and to be targeted to the cell surface, leading to the suggestion that dimerization could play a role in the ER quality control system of newly synthesized proteins and their export to the cell surface. Similar propositions were made following the observation that mutations in TM1 and TM4, which prevented α_{1b}AR dimerization, led to ER retention (19,20). Such a role for oligomerization in the ER quality control of GPCRs would not be surprising because protein–protein interactions, including both homo- and heterodimerization, have often been shown to play prominent roles in the quality control of many proteins (68).

One of the difficulties in establishing a causal link between dimerization and receptor trafficking from mutagenesis study is to exclude the possibility that both the loss in dimerization and cell surface targeting may result from misfolding of the receptor caused by the mutation and thus may not indicate a causal relationship between dimerization and trafficking, both dimerization and cell surface trafficking being independently affected by the conformational change imposed by the mutations.

The ability of lipophilic ligands to favor the folding and cell surface expression of ER-retained proteins has been previously shown for several GPCRs and is referred to as pharmacological chaperoning (42). Pharmacological chaperones bind to ER-retained proteins and favor their escape from the ER quality control system, allowing trafficking to their proper site of action. It is believed that ER-retained proteins that can be rescued by pharmacological chaperones bear relatively modest mutations that, although recognized by the quality control systems as improperly or incompletely folded, can still reach near-native conformations that are stabilized by the binding of the pharmacological chaperone; hence, their release from the ER. Alprenolol clearly acted as a pharmacological chaperone on W183Aβ_1AR as it promoted receptor maturation from its ER-located core-glycosylated form to fully glycosylated species, reflecting Golgi processing and resulting in cell surface targeting. Interestingly, this action of alprenolol correlated with a restoration of the receptor's propensity to self-assemble, as reflected by the time-dependent reduction in $BRET_{50}$ observed upon alprenolol treatment. The effects of alprenolol on dimerization and cell surface expression had similar kinetics that are consistent with pharmacological chaperoning. The link between the pharmacological chaperoning effect of alprenolol and its ability to promote receptor dimerization is further supported by the observation that alprenolol promotes dimerization while the receptor is still in the ER. Indeed, brefeldin A treatment, which prevents ER exit, did not block the alprenolol-induced decrease in W183Aβ_1AR $BRET_{50}$. The good correlation between the lipophilic character of the various βAR ligands tested and their ability to restore β_1AR self-assembly is also compatible with the notion that they need to penetrate biological membranes to have their action in the ER. Collectively, these findings are consistent with many other studies indicating that GPCR oligomerization occurs early after biosynthesis, most likely in the ER (17). During the revision of the present manuscript, a study reported that α-adrenergic ligands that act as pharmacological chaperones for the cell surface targeting of ER-retained α_{1B}AR mutants also restored receptor homodimerization (20), suggesting that action of pharmacological chaperone on receptor self-assembly may be a general feature of pharmacological chaperone action.

How pharmacological chaperones restores dimerization of the receptor remains to be determined. Given that the W183A mutation was found to reduce but not abolish the propensity of the β_1AR to self-assemble and that the effect may result either from a local misfolding of the receptor or from a direct effect on the dimerization interface, two possible and non-exclusive models can be proposed: (i) the pharmacological chaperone binds to a monomeric form of the receptor that has a reduced propensity to dimerize, as a result of a local misfolding promoted by the mutations, and stabilizes a near-native conformation of the receptor that can now dimerize more readily and (ii) the pharmacological chaperone binds to a dimeric receptor form that has been destabilised by the mutations and, through ligand binding energy, stabilizes the dimeric complex, hence driving the monomer/dimer equilibrium towards dimerization. These two possibilities are difficult to differentiate experimentally with the currently available techniques. Dimerization can also be seen as a component of the overall receptor folding, making it even more difficult to distinguish effects that are specific to the dimerization process. Whether the dimerization-promoting action of the pharmacological chaperones is part of their mode of action to promote ER-export of the receptor or simply a consequence of the stabilization of the receptor's native conformation also remains to be determined. Nevertheless, we can conclude that alprenolol has positive effects on both homodimerization and ER-export of the

receptor, thus linking the two phenomena in a gain of function paradigm.

The sequence of events linking folding, dimerization and ER-export as well as the precise mode of action of the pharmacological chaperone still remains to be clarified.

Materials and Methods

Materials

Dulbecco's modified Eagle's medium, penicillin–streptomycin, L-glutamine and phosphate-buffered saline (PBS) were obtained from Wisent. Leupeptin, benzamidine, soybean trypsin inhibitor, Phenylmethanesulfonyl fluoride, (-)-alprenolol, (-)-isoproterenol, dobutamine, S-(-)-atenolol, (±)-metoprolol, DL-propranolol and labetalol were purchased from Sigma-Aldrich. Carvedilol is a generous gift from GlaxoSmithKline. DeepBlueC coelenterazine was purchased from Biotium Inc. Coelenterazine h was purchased from Nanolight Technology. Brefeldin A was purchased from Calbiochem. Horseradish peroxidase-conjugated rat anti-HA antibody (3F10) and FuGENE6 were obtained from Roche diagnostics GmbH. Mouse anti-calnexin antibody was purchased from BD biosciences. Mouse anti-HA (12CA5) and anti-myc (9E10) antibodies were produced in our core facility as ascitic fluids.

ET analysis of β_1AR

The evolutionary importance was calculated by ET (69) from sequences of TM domain of 139 bioamine receptors, which consist of 29 α-adrenergic, 26 β-adrenergic, 30 serotonergic, 30 dopaminergic, 18 cholinergic and 6 histaminic receptors. Protein sequences corresponding to TM domains, TM1 (Trp35 to Gln64), TM2 (Pro71 to His100), TM3 (Pro107 to Val139), TM4 (Asn151 to Val173), TM5 (Asn200 to Gln225), TM6 (Glu247 to Thr277), and TM7 (Ile286 to Tyr306) of bovine rhodopsin (Swissprot: OPSD_BOVIN), were analyzed. Among the residues ranking in top 50%, structural clusters located on the protein surface were picked up as candidates of dimerization interfaces. An ET server is available at http://mammoth.bcm.tmc.edu/.

Receptor constructs

Vectors encoding β_1AR-GFP10, β_1AR-*R*luc and β_2AR-*R*luc have been described previously (55). In order to construct N-terminally HA-tagged β_1AR (HA-β_1AR) and myc-tagged β_2AR (myc-β_2AR), βAR sequence was amplified using a primer harboring the Kozak and Hemagglutinin Tag (YPYDVPDYA) or c-myc Epitope Tag (EQKLISEEDL) sequences, and subcloned into pcDNA3.1/Zeo (+). β_1AR-eGFP was obtained from β_1AR-GFP10 by subcloning the coding sequence of β_1AR into pEGFP-N1 expression vector (Clontech). β_1AR-Venus and β_2AR-Venus were created by exchanging the C-terminal-fused fluorophore of β_2AR-GFP10 (55) with the Venus variant of eYFP (70). HA-β_1AR-*R*luc, HA-β_1AR-Venus, and myc-β_2AR-Venus, which were used in the analysis of cell surface receptor expression, were created by replacing the N-terminal region of *R*luc- or Venus-fused constructs with the corresponding coding sequence of HA- or myc-tagged constructs. Mutant β_1ARs (L105F, I194W, V179W, W183F and W183A) were created using QuikChange XL site-directed mutagenesis kit (Stratagene).

Cell culture and transfection

HEK293 cells were maintained in Dulbecco's modified Eagle's medium supplemented with 5% fetal bovine serum, 100 units/ml penicillin and 100 µg/ml streptomycin at 37°C in a humidified atmosphere, with 5% CO_2. Transient transfections were performed using FuGENE6, according to the manufacturer's protocol. Cells were harvested 48 h after transfection to perform the indicated assay.

BRET^2 assay

BRET assay was carried out as previously described (71). Briefly, HEK293 cells resuspended in PBS were distributed in 96-well microplate (Corning No. 3917). The luciferase substrate, DeepBlueC coelenterazine, was added at a final concentration of 5 µM. Signals were detected at 370–450 nm and 500–530 nm using a modified TopCount NXT plate reader (Packard Bioscience) equipped with the appropriate band pass filters. BRET signals were calculated as the ratio of the light emitted by GFP10 (500–530 nm) over the light emitted by *R*luc (370–450 nm). The expression level of the energy acceptor (GFP10) tagged proteins were measured as total fluorescence using a FluoroCount fluorometer (Packard) with an excitation filter at 400 nm and an emission filter at 510 nm. The expression level of the energy donor (*R*luc) tagged protein was measured using a LumiCount luminometer (Packard) in the presence of 5 µM coelenterazine h. BRET signals were drawn as a function of the GFP10/*R*luc total expression ratio, as previously described (55). $BRET_{50}$ values were identified as the GFP/*R*luc ratio leading to 50% of the maximal BRET.

Confocal microscopy

HEK293 cells were plated on poly-D-lysine coated coverslips and transfected with the indicated plasmids; 48 h after transfection, coverslips were washed with PBS and fixed with 3% paraformaldehyde for 15 min. Receptor distribution was generally assessed by direct fluorescence detection of the fused eGFP or Venus in non-permeabilized cells. When indicated, cells were permeabilized with PBS containing 0.2% BSA and 0.3% triton-X100 for 10 min followed by immunolabeling using mouse anti-calnexin (1:100) as primary antibody and Alexa Fluor 594 conjugated goat anti-mouse immunoglobulin (IgG) as secondary antibody. Confocal microscopy images were obtained using a Zeiss LSM510 META laser scanning microscope. Laser excitation and emission filters used were as follows: eGFP: $\lambda_{ex} = 488$ nm, $\lambda_{em} = 505–530$ nm; Venus: $\lambda_{ex} = 514$ nm, $\lambda_{em} = 530–600$ nm; Alexa Fluor 594: $\lambda_{ex} = 543$ nm, $\lambda_{em} = 575–630$ nm.

Cell surface receptor expression assay (fixed cells)

HEK293 cells were plated on poly-D-lysine coated dishes, transfected with WT or W183A mutant HA-β_1AR-*R*luc and treated or not with 10 µM alprenolol for 4 or 24 h, prior to measurement. To determine receptor cell surface expression, cells were washed twice with PBS, blocked with PBS containing 1% bovine serum albumin, and labeled with mouse anti-HA antibody (1:1000). Cells were then washed with PBS, fixed with 3% paraformaldehyde and cell surface expression level detected using horseradish peroxidase-conjugated anti-mouse IgG antibody (1:1000) and SIGMA FAST™ o-phenylenediamine dihydrochloride peroxidase substrate kit. From the same batch of cells, total receptor expression level was determined by measuring total luminescence in the presence of 5 µM coelenterazine h using a LumiCount reader (Packard). Cell surface receptor expression was determined as the ratio of cell surface over total expression.

Cell surface receptor expression assay (non-fixed cells)

HEK293 cells were co-transfected with HA-WTβ_1AR-Venus or myc-WTβ_2AR-Venus, with or without W183Aβ_1AR. To determine WT receptor cell surface expression, cells were detached, resuspended in PBS and labeled with mouse anti-HA antibody (1:1000) or mouse anti-myc antibody (1:1000). Cells were then washed with PBS and cell surface expression level detected using horseradish peroxidase-conjugated anti-mouse IgG antibody (1:1000) and SIGMA FAST™ o-phenylenediamine dihydrochloride peroxidase substrate kit. Total receptor expression level was determined by measuring Venus fluorescence. In order to exclude the effect on expression level of W183Aβ_1AR co-expression, cell surface receptor expression was determined as the ratio of cell surface over total expression and expressed as a percentage of surface expression level estimated from a regression curve using surface expression and total expression in the absence of W183Aβ_1AR.

Intracellular cAMP measurement

cAMP accumulation in living cells was determined by ELISA based assay using CatchPoint™ cAMP assay kit (Molecular Devices, CA). In brief, HEK293 cells were transfected with WT or W183A mutant β_1AR, and treated or not with 10 µM alprenolol for 16 h. Cells were then detached in PBS containing 0.5 mM EDTA and washed extensively with PBS.

Cells (5×10^3 cells) were incubated with increasing concentrations of dobutamine, a selective β_1AR agonist, for 15 min at 37°C in phosphate-buffered saline containing 10 mM glucose and 750 μM 3-isobutyl-1-methyl-xanthine. cAMP production was determined according to standard kit protocol and detected as fluorescence (excitation 530 nm and emission 590 nm) using the Flex-Station II microplate reader (Molecular Devices).

Deglycosylation assay of β_1AR

HEK293 cells transfected with WT or W183A mutant were solubilized in 85 mM NaCl, 75 mM Tris–HCl pH 7.4, 12.5 mM $MgCl_2$, 0.5 % N-dodecyl maltoside, 5 μg/ml leupeptin, 10 μg/ml benzamidine, and 5 μg/ml soybean trypsin inhibitor. Samples were sonicated and centrifuged at 5000 × g for 5 min. Supernatants were immunoprecipitated using anti-HA antibody (12CA5 1:100) and protein G-sepharose overnight at 4°C. The immune complex were pelleted by brief centrifugation, washed twice with solubilization buffer, and resuspended into assay buffer (50 mM sodium phosphate pH 5.5, 50 mM EDTA, 1% 2-mercaptoethanol, 0.5% N-dodecyl maltoside, 0.2 mM Phenylmethanesulfonyl fluoride, 5 μg/ml leupeptin, 10 μg/ml benzamidine and 5 μg/ml soybean trypsin inhibitor). Samples were incubated 24 h at 37°C in the presence or absence of endoH (1 unit/sample) and separated onto 10% SDS-PAGE. Resolved proteins were transferred to nitrocellulose membrane and blotted with horseradish peroxidase-conjugated 3F10 anti-HA antibody (1:1000). Western blots were developed using Western Lightning™ ECL kit (PerkinElmer).

Data analysis

ClogP (hydrophobicity partition coefficient) values of β-adrenergic ligands were calculated by Daylight (Chemical Information Systems, Inc). Statistical analysis was carried out using Prism (GraphPad software). $BRET_{50}$ values of BRET titration assay were calculated using single site binding model. Statistical comparison were made using paired Student's *t*-test for the comparisons between two groups or one-way analysis of variance followed by Dunnett's test for multiple comparisons. Correlation between samples was estimated with Pearson's product-moment correlation coefficient. The statistical significance of the differences between the $BRET_{50}$ after different times of treatment with alprenolol was determined by *F* tests of non-linear regression of each BRET titration curves compared with the non-treated condition after Bonferroni corrections for multiple comparison.

Acknowledgments

The authors are grateful to Dr Monique Lagacé for her critical reading of the manuscript, Dr Céline Galés for expert opinion in BRET experiments, Martin Audet for useful discussion on receptor crystal structure and Monique Vasseur for technical assistance in fluorescence microscopy studies. We thank GlaxoSmithKline (Research Triangle Park, NC) for their generous gift of carvedilol and Dr Shigeru Furukubo from Tanabe Seiyaku Co. Ltd for the determination of ClogP of β-adrenergic ligands. K. O. was an invited researcher from Tanabe Seiyaku Co. Ltd. M. B. holds a Canada Research Chair in Signal Transduction and Molecular Pharmacology. This work was supported by grant GM066099 given to O. L. from the NIH and also supported by operating grant FRN-11215 and team grant CTP-79848 from the Canadian Institute for Health Research, and grant from the Heart and Stroke Foundation of Canada given to M. B.

Supporting Information

Additional Supporting Information may be found in the online version of this article:

Table S1: List of monoamine GPCR sequences used for ET analysis

Figure S1: Homodimerization BRET competition. Cells were co-transfected with fixed amount of WTβ_1AR-*R*luc and increasing amounts of WTβ_1AR-GFP10, in the presence or absence of HA-β_1AR as BRET competitor; 0, 0.1 or 0.5 μg HA-β_1AR was transfected whereas the amounts of WTβ_1AR-GFP10 construct were ranging from 0.02 to 0.5 μg. Expression of the HA-β_1AR BRET competitor leads to a decrease in maximal BRET and a rightward shift in $BRET_{50}$ values ($BRET_{50}$ values: no competitor, 0.36; 0.1 μg competitor, 0.75; and 0.5 μg competitor, 1.9). The BRET partners expression levels were as followed: in the absence of competitor, WTβ_1AR-*R*luc: 1006–2133 fmol and WTβ_1AR-GFP10: 333–1223 fmol; in the presence of 0.1 μg competitor, WTβ_1AR-*R*luc: 856–1914 fmol and WTβ_1AR-GFP10: 139–906 fmol; in the presence of 0.5 μg competitor, WTβ_1AR-*R*luc: 499–806 fmol and WTβ_1AR-GFP10: 60–545 fmol. Although the expression of HA-β_1AR at the highest concentration (0.5 μg) resulted in a significant decrease in the absolute amount of WTβ_1AR-*R*luc and WTβ_1AR-GFP10, the reduced BRET did not result from lower expression of the BRET partners because equally low levels of BRET partners did not yield similarly blunted BRET in the absence of BRET competitor (data not shown)

Figure S2: Additive effect of V179W and W183A mutation on the inhibition of β_1AR homodimerization. Cells were co-transfected with fixed amount of β_1AR-*R*luc and increasing amounts of β_1AR-GFP10. In each experiment, the *R*luc- and GFP10-fused constructs are carrying identical mutations (either V179W/W183A or W183A). Whereas titration with W183A β_1AR led to a saturable BRET curve, the BRET values obtained for V179W/W183Aβ_1AR did not converge to an asymptote, indicative of a non-specific signal resulting from bystander BRET

Figure S3: Correlation between receptor number and fluorescence or luminescence signals. Increasing concentrations of WT and mutant β_1AR-*R*luc or β_1AR-GFP10 constructs were transfected in HEK293 cells. Total fluorescence or luminescence signal as well as [^{3}H]-dihydroalprenolol binding were determined. Although the absolute level of expression varied among different mutants, unique linear correlations were observed between the number of sites detected by radioligand binding and both the fluorescence ($r^2 = 0.78$) and luminescence ($r^2 = 0.79$) signals. Such standard curves were used to transform fluorescence and luminescence values into receptor numbers

Figure S4: Distribution of the expression levels for WT and mutant β_1AR-*R*luc or β_1AR-GFP10. Expression level (RLU, RFU) were derived by transforming the total fluorescence and luminescence signals into receptor numbers using standard curves such as those presented in Figure S3. Each data point corresponds to a point in the BRET titration curves shown in Figure 2A

Figure S5: Homodimerization BRET competition with β_2AR. Cells were co-transfected with fixed amount of WTβ_1AR-*R*luc and increasing amounts of WTβ_1AR-GFP10 in the presence and absence of HA-β_2AR as BRET competitor; 0, 0.003, 0.1 or 0.3 μg HA-β_2AR was transfected whereas the amounts of WTβ_1AR-GFP10 construct were ranging from 0.02 to 0.5 μg. Expression of the HA-β_2AR BRET competitor did not significantly change BRET signals between WTβ_1AR-*R*luc and WTβ_1AR-GFP10

Please note: Wiley-Blackwell are not responsible for the content or functionality of any supporting materials supplied by the authors. Any queries (other than missing material) should be directed to the corresponding author for the article.

References

1. Petäjä-Repo UE, Hogue M, Laperrière A, Walker P, Bouvier M. Export from the endoplasmic reticulum represents the limiting step in the maturation and cell surface expression of the human δ opioid receptor. J Biol Chem 2000;275:13727–13736.

2. Dong C, Filipeanu CM, Duvernay MT, Wu G. Regulation of G protein-coupled receptor export trafficking. Biochim Biophys Acta 2007; 1768:853–870.
3. Lanctôt PM, Leclerc PC, Escher E, Guillemette G, Leduc R. Role of N-glycan-dependent quality control in the cell-surface expression of the AT1 receptor. Biochem Biophys Res Commun 2006;340:395–402.
4. Mizrachi D, Segaloff DL. Intracellularly located misfolded glycoprotein hormone receptors associate with different chaperone proteins than their cognate wild-type receptors. Mol Endocrinol 2004;18: 1768–1777.
5. Morello JP, Salahpour A, Petäjä-Repo UE, Laperrière A, Lonergan M, Arthus MF, Nabi IR, Bichet DG, Bouvier M. Association of calnexin with wild type and mutant AVPR2 that causes nephrogenic diabetes insipidus. Biochemistry 2001;40:6766–6775.
6. Rosenbaum EE, Hardie RC, Colley NJ. Calnexin is essential for rhodopsin maturation, Ca^{2+} regulation, and photoreceptor cell survival. Neuron 2006;49:229–241.
7. Rozell TG, Davis DP, Chai Y, Segaloff DL. Association of gonadotropin receptor precursors with the protein folding chaperone calnexin. Endocrinology 1998;139:1588–1593.
8. Siffroi-Fernandez S, Giraud A, Lanet J, Franc JL. Association of the thyrotropin receptor with calnexin, calreticulin and BiP. Effects on the maturation of the receptor. Eur J Biochem 2002;269:4930–4937.
9. Baker EK, Colley NJ, Zuker CS. The cyclophilin homolog NinaA functions as a chaperone, forming a stable complex in vivo with its protein target rhodopsin. EMBO J 1994;13:4886–4895.
10. Ferreira PA, Nakayama TA, Pak WL, Travis GH. Cyclophilin-related protein RanBP2 acts as chaperone for red/green opsin. Nature 1996; 383:637–640.
11. Héroux M, Hogue M, Lemieux S, Bouvier M. Functional calcitonin gene-related peptide receptors are formed by the asymmetric assembly of a calcitonin receptor-like receptor homo-oligomer and a monomer of receptor activity-modifying protein-1. J Biol Chem 2007; 282:31610–31620.
12. Hilairet S, Belanger C, Bertrand J, Laperriere A, Foord SM, Bouvier M. Agonist-promoted internalization of a ternary complex between calcitonin receptor-like receptor, receptor activity-modifying protein 1 (RAMP1), and beta-arrestin. J Biol Chem 2001;276:42182–42190.
13. Loconto J, Papes F, Chang E, Stowers L, Jones EP, Takada T, Kumánovics A, Fischer Lindahl K, Dulac C. Functional expression of murine V2R pheromone receptors involves selective association with the M10 and M1 families of MHC class Ib molecules. Cell 2003; 112:607–618.
14. McLatchie LM, Fraser NJ, Main MJ, Wise A, Brown J, Thompson N, Solari R, Lee MG, Foord SM. RAMPs regulate the transport and ligand specificity of the calcitonin-receptor-like receptor. Nature 1998; 393:333–339.
15. Parameswaran N, Spielman WS. RAMPs: the past, present and future. Trends Biochem Sci 2006;31:631–638.
16. Marshall FH, Jones KA, Kaupmann K, Bettler B. $GABA_B$ receptors – the first 7TM heterodimers. Trends Pharmacol Sci 1999;20: 396–399.
17. Bulenger S, Marullo S, Bouvier M. Emerging role of homo- and heterodimerization in G-protein-coupled receptor biosynthesis and maturation. Trends Pharmacol Sci 2005;26:131–137.
18. Salahpour A, Angers S, Mercier JF, Lagacé M, Marullo S, Bouvier M. Homodimerization of the β_2-adrenergic receptor as a prerequisite for cell surface targeting. J Biol Chem 2004;279:33390–33397.
19. Lopez-Gimenez JF, Canals M, Pediani JD, Milligan G. The α_{1b}-adrenoceptor exists as a higher-order oligomer: effective oligomerization is required for receptor maturation, surface delivery, and function. Mol Pharmacol 2007;71:1015–1029.
20. Canals M, Lopez-Gimenez JF, Milligan G. Cell surface delivery and structural re-organization by pharmacological chaperones of an oligomerization-defective α_{1b}-adrenoceptor mutant demonstrates membrane targeting of GPCR oligomers. Biochem J 2009;417:161–172.
21. Hague C, Uberti MA, Chen Z, Hall RA, Minneman KP. Cell surface expression of α_{1D}-adrenergic receptors is controlled by heterodimerization with α_{1B}-adrenergic receptors. J Biol Chem 2004;279:15541–15549.
22. Uberti MA, Hague C, Oller H, Minneman KP, Hall RA. Heterodimerization with β_2-adrenergic receptors promotes surface expression and functional activity of α_{1D}-adrenergic receptors. J Pharmacol Exp Ther 2005;313:16–23.
23. Guo W, Shi L, Filizola M, Weinstein H, Javitch JA. Crosstalk in G protein-coupled receptors: changes at the transmembrane homodimer interface determine activation. Proc Natl Acad Sci USA 2005;102:17495–17500.
24. Guo W, Shi L, Javitch JA. The fourth transmembrane segment forms the interface of the dopamine D2 receptor homodimer. J Biol Chem 2003;278:4385–4388.
25. Carrillo JJ, Lopez-Gimenez JF, Milligan G. Multiple interactions between transmembrane helices generate the oligomeric $alpha_{1b}$-adrenoceptor. Mol Pharmacol 2004;66:1123–1137.
26. Hebert TE, Moffett S, Morello JP, Loisel TP, Bichet DG, Barret C, Bouvier M. A peptide derived from a β_2-adrenergic receptor transmembrane domain inhibits both receptor dimerization and activation. J Biol Chem 1996;271:16384–16392.
27. Lee SP, O'Dowd BF, Rajaram RD, Nguyen T, George SR. D2 dopamine receptor homodimerization is mediated by multiple sites of interaction, including an intermolecular interaction involving transmembrane domain 4. Biochemistry 2003;42:11023–11031.
28. Hernanz-Falcón P, Rodrïguez-Frade JM, Serrano A, Juan D, del Sol A, Soriano SF, Roncal F, Gómez L, Valencia A, Martïnez AC, Mellado M. Identification of amino acid residues crucial for chemokine receptor dimerization. Nat Immunol 2004;5:216–223.
29. Overton MC, Chinault SL, Blumer KJ. Oligomerization, biogenesis, and signaling is promoted by a glycophorin A-like dimerization motif in transmembrane domain 1 of a yeast G protein-coupled receptor. J Biol Chem 2003;278:49369–49377.
30. Lichtarge O, Bourne HR, Cohen FE. An evolutionary trace method defines binding surfaces common to protein families. J Mol Biol 1996; 257:342–358.
31. Lichtarge O, Sowa ME. Evolutionary predictions of binding surfaces and interactions. Curr Opin Struct Biol 2002;12:21–27.
32. Raviscioni M, He Q, Salicru EM, Smith CL, Lichtarge O. Evolutionary identification of a subtype specific functional site in the ligand binding domain of steroid receptors. Proteins 2006;64:1046–1057.
33. Shenoy SK, Drake MT, Nelson CD, Houtz DA, Xiao K, Madabushi S, Reiter E, Premont RT, Lichtarge O, Lefkowitz RJ. β-arrestin-dependent, G protein-independent ERK1/2 activation by the β_2 adrenergic receptor. J Biol Chem 2006;281:1261–1273.
34. Reš I, Lichtarge O. Character and evolution of protein-protein interfaces. Phys Biol 2005;2:S36–S43.
35. Sowa ME, He W, Slep KC, Kercher MA, Lichtarge O, Wensel TG. Prediction and confirmation of a site critical for effector regulation of RGS domain activity. Nat Struct Biol 2001;8:234–237.
36. Yang M, Wang W, Zhong M, Philippi A, Lichtarge O, Sanborn BM. Lysine 270 in the third intracellular domain of the oxytocin receptor is an important determinant for G alpha(q) coupling specificity. Mol Endocrinol 2002;16:814–823.
37. Lin CY, Varma MG, Joubel A, Madabushi S, Lichtarge O, Barber DL. Conserved motifs in somatostatin, D2-dopamine, and alpha 2B-adrenergic receptors for inhibiting the Na-H exchanger, NHE1. J Biol Chem 2003;278:15128–15135.
38. Quan XJ, Denayer T, Yan J, Jafar-Nejad H, Philippi A, Lichtarge O, Vleminckx K, Hassan BA. Evolution of neural precursor selection:

functional divergence of proneural proteins. Development 2004; 131:1679–1689.
39. Raviscioni M, Gu P, Sattar M, Cooney AJ, Lichtarge O. Correlated evolutionary pressure at interacting transcription factors and DNA response elements can guide the rational engineering of DNA binding specificity. J Mol Biol 2005;350:402–415.
40. Ribes-Zamora A, Mihalek I, Lichtarge O, Bertuch AA. Distinct faces of the Ku heterodimer mediate DNA repair and telomeric functions. Nat Struct Mol Biol 2007;14:301–307.
41. Bernier V, Bichet DG, Bouvier M. Pharmacological chaperone action on G-protein-coupled receptors. Curr Opin Pharmacol 2004;4: 528–533.
42. Bernier V, Lagace M, Bichet DG, Bouvier M. Pharmacological chaperones: potential treatment for conformational diseases. Trends Endocrinol Metab 2004;15:222–228.
43. Bernier V, Morello JP, Zarruk A, Debrand N, Salahpour A, Lonergan M, Arthus MF, Laperrière A, Brouard R, Bouvier M, Bichet DG. Pharmacologic chaperones as a potential treatment for X-linked nephrogenic diabetes insipidus. J Am Soc Nephrol 2006;17: 232–243.
44. Conn PM, Ulloa-Aguirre A, Ito J, Janovick JA. G protein-coupled receptor trafficking in health and disease: lessons learned to prepare for therapeutic mutant rescue in vivo. Pharmacol Rev 2007;59:225–250.
45. Madabushi S, Yao H, Marsh M, Kristensen DM, Philippi A, Sowa ME, Lichtarge O. Structural clusters of evolutionary trace residues are statistically significant and common in proteins. J Mol Biol 2002; 316:139–154.
46. Mihalek I, Reš I, Lichtarge O. A family of evolution-entropy hybrid methods for ranking protein residues by importance. J Mol Biol 2004;336:1265–1282.
47. Madabushi S, Gross AK, Philippi A, Meng EC, Wensel TG, Lichtarge O. Evolutionary trace of G protein-coupled receptors reveals clusters of residues that determine global and class-specific functions. J Biol Chem 2004;279:8126–8132.
48. Allman K, Page KM, Curtis CA, Hulme EC. Scanning mutagenesis identifies amino acid side chains in transmembrane domain 5 of the M_1 muscarinic receptor that participate in binding the acetyl methyl group of acetylcholine. Mol Pharmacol 2000;58:175–184.
49. Kostenis E, Conklin BR, Wess J. Molecular basis of receptor/G protein coupling selectivity studied by coexpression of wild type and mutant m_2 muscarinic receptors with mutant G alpha(q) subunits. Biochemistry 1997;36:1487–1495.
50. Peltonen JM, Nyronen T, Wurster S, Pihlavisto M, Hoffren AM, Marjamaki A, Xhaard H, Kanerva L, Savola JM, Johnson MS, Scheinin M. Molecular mechanisms of ligand-receptor interactions in transmembrane domain V of the alpha2A-adrenoceptor. Br J Pharmacol 2003;140:347–358.
51. Schmidt C, Li B, Bloodworth L, Erlenbach I, Zeng FY, Wess J. Random mutagenesis of the M_3 muscarinic acetylcholine receptor expressed in yeast. Identification of point mutations that ''silence'' a constitutively active mutant M_3 receptor and greatly impair receptor/G protein coupling. J Biol Chem 2003;278:30248–30260.
52. Shapiro DA, Kristiansen K, Kroeze WK, Roth BL. Differential modes of agonist binding to 5-hydroxytryptamine(2A) serotonin receptors revealed by mutation and molecular modeling of conserved residues in transmembrane region 5. Mol Pharmacol 2000;58:877–886.
53. Wurch T, Colpaert FC, Pauwels PJ. Chimeric receptor analysis of the ketanserin binding site in the human 5-Hydroxytryptamine1D receptor: importance of the second extracellular loop and fifth transmembrane domain in antagonist binding. Mol Pharmacol 1998;54:1088–1096.
54. Prasher DC, Eckenrode VK, Ward WW, Prendergast FG, Cormier MJ. Primary structure of the Aequorea victoria green-fluorescent protein. Gene 1992;111:229–233.
55. Mercier JF, Salahpour A, Angers S, Breit A, Bouvier M. Quantitative assessment of β_1- and β_2-adrenergic receptor homo- and heterodimerization by bioluminescence resonance energy transfer. J Biol Chem 2002;277:44925–44931.
56. Terrillon S, Durroux T, Mouillac B, Breit A, Ayoub MA, Taulan M, Jockers R, Barberis C, Bouvier M. Oxytocin and vasopressin V1a and V2 receptors form constitutive homo- and heterodimers during biosynthesis. Mol Endocrinol 2003;17:677–691.
57. Dickinson KE, Heald SL, Jeffs PW, Lefkowitz RJ, Caron MG. Covalent labeling of the β-adrenergic ligand-binding site with para-(bromoacetamidyl)benzylcarazolol. A highly potent beta-adrenergic affinity label. Mol Pharmacol 1985;27:499–506.
58. Morello JP, Salahpour A, Laperriere A, Bernier V, Arthus MF, Lonergan M, Petaja-Repo U, Angers S, Morin D, Bichet DG, Bouvier M. Pharmacological chaperones rescue cell-surface expression and function of misfolded V2 vasopressin receptor mutants. J Clin Invest 2000;105:887–895.
59. Petäjä-Repo UE, Hogue M, Bhalla S, Laperrière A, Morello JP, Bouvier M. Ligands act as pharmacological chaperones and increase the efficiency of δ opioid receptor maturation. EMBO J 2002;21:1628–1637.
60. Guo W, Urizar E, Kralikova M, Mobarec JC, Shi L, Filizola M, Javitch JA. Dopamine D2 receptors form higher order oligomers at physiological expression levels. EMBO J 2008;27:2293–2304.
61. Hamatake M, Aoki T, Futahashi Y, Urano E, Yamamoto N, Komano J. Ligand-independent higher-order multimerization of CXCR4, a G-protein-coupled chemokine receptor involved in targeted metastasis. Cancer Sci 2009;100:95–102.
62. Warne T, Serrano-Vega MJ, Baker JG, Moukhametzianov R, Edwards PC, Henderson R, Leslie AG, Tate CG, Schertler GF. Structure of a beta1-adrenergic G-protein-coupled receptor. Nature 2008; 454:486–491.
63. Milligan G. A day in the life of a G protein-coupled receptor: the contribution to function of G protein-coupled receptor dimerization. Br J Pharmacol 2008;153:Suppl 1): S216–S229.
64. Davies A, Gowen BE, Krebs AM, Schertler GF, Saibil HR. Three-dimensional structure of an invertebrate rhodopsin and basis for ordered alignment in the photoreceptor membrane. J Mol Biol 2001;314:455–463.
65. Liang Y, Fotiadis D, Filipek S, Saperstein DA, Palczewski K, Engel A. Organization of the G protein-coupled receptors rhodopsin and opsin in native membranes. J Biol Chem 2003;278:21655–21662.
66. Sánchez-Laorden BL, Sánchez-Más J, Martïnez-Alonso E, Martïnez-Menárguez JA, Garcïa-Borrón JC, Jiménez-Cervantes C. Dimerization of the human melanocortin 1 receptor: functional consequences and dominant-negative effects. J Invest Dermatol 2006;126:172–181.
67. Herrick-Davis K, Grinde E, Harrigan TJ, Mazurkiewicz JE. Inhibition of serotonin 5-hydroxytryptamine$_{2c}$ receptor function through heterodimerization: receptor dimers bind two molecules of ligand and one G-protein. J Biol Chem 2005;280:40144–40151.
68. Ma D, Jan LY. ER transport signals and trafficking of potassium channels and receptors. Curr Opin Neurobiol 2002;12:287–292.
69. Yao H, Kristensen DM, Mihalek I, Sowa ME, Shaw C, Kimmel M, Kavraki L, Lichtarge O. An accurate, sensitive, and scalable method to identify functional sites in protein structures. J Mol Biol 2003; 326:255–261.
70. Nagai T, Ibata K, Park ES, Kubota M, Mikoshiba K, Miyawaki A. A variant of yellow fluorescent protein with fast and efficient maturation for cell-biological applications. Nat Biotechnol 2002;20:87–90.
71. Galés C, Van Durm JJ, Schaak S, Pontier S, Percherancier Y, Audet M, Paris H, Bouvier M. Probing the activation-promoted structural rearrangements in preassembled receptor-G protein complexes. Nat Struct Mol Biol 2006;13:778–786.